Supporting Information

Hassani *et al.* 10.1073/pnas.0811400106

SI Methods: Detailed Procedures

Animals and Surgery. All procedures were approved by the McGill University Animal Care Committee and the Canadian Council on Animal Care. Adult Long–Evans rats (200–250 g, Charles River) were operated on under deep anesthesia (ketamine, xylazine, and acepromazine: 65:5:1 mg/kg in a mixture of 2 mL/kg initial dose and 1 mg/kg booster as needed, i.p.). EEG [epidural screws over cortex, including olfactory bulb (OB), anterior medial prefrontal cortex (PF), and retrosplenial cortex (RS)], and EMG electrodes (silver wire loops in neck muscles) were implanted together with a metal u-frame for holding the head by screws to a sliding carriage adapter within the stereotaxic frame, as described in ref. 1. Animals were maintained on a 12:12 h light-dark schedule with lights on from 700 to 1900 h. Under control conditions, they were given free access to food and water when not in the recording chamber (see below). After recovery from surgery (≈2 days), they were gradually habituated to remain quiet with their heads fixed in the carriage adapter while lying within a small Plexiglas box, which prevented twisting but not moving their bodies and limbs. After adaptation (6–9 days), the rats were once again anesthetized (as above) and operated on for drilling holes in the skull (AP −2.8 mm from bregma, L ± 1.3 mm) and opening the dura over the lateral hypothalamic area on each side. After 1 day of recovery, daily recording sessions of <6 h (≈1100–1700 h) were performed over a maximum of 4 days.

Unit Recording and Labeling. Single units were recorded by using glass micropipettes (≈1-μm tip) that were filled with 0.5 M NaCl and ≈5% Neurobiotin (Nb, Vector Laboratories) and an intracellular amplifier (Neurodata IR-283A, Cygnus Technology). The unit signal was amplified (×2,000) and filtered (0.3–3 kHz) by using a CyberAmp380 (Axon Instruments), then acquired at 16 kHz for on-line viewing with Axoscope (v8.1, Axon Instruments). The unit signal and EEG/EMG were simultaneously acquired and digitized at 8 kHz and 250 Hz, respectively, by using EEG and sleep-waking scoring software (Harmonie v5.2, Stellate Co.). Video recording of behavior was also acquired simultaneously by the same software. On the last day of recording from one side, the last cell recorded during aW, SWS, and PS was labeled with Nb by using the juxtacellular technique, as described in refs. 2 and 3. It was estimated that ≈80% of units submitted to the juxtacellular labeling protocol were successfully labeled with Nb (for a total of 117 cells labeled in 75 rats).

Feeding Conditions. Under normal conditions, rats were given free access to food and water when not in the recording box. After the recording and successful labeling of 62 units from 40 rats among which none were found to be MCH+, feeding conditions were altered in an effort to maximize the probability of finding discharging MCH+ neurons. In previous in vivo studies, food restriction was reported to stimulate cAMP response element-binding protein-dependent pathways in MCH neurons (4), potentially reflecting their increased activity. A food restriction regime was thus imposed according to which animals received only 6 g of food pellets the night preceding the recording. One cell of 22 successfully labeled cells in 13 rats thus treated was identified as MCH+. A reverse approach was subsequently tried based on in vitro results showing that MCH neurons discharge in response to high concentrations (≥5 mM) of glucose (5). Rats were thus given a sucrose solution (2 g/kg) for oral ingestion 5 min before the beginning of the recording session, a protocol

shown to induce an increase in cerebral glucose concentration (6, 7). One cell of 6 cells successfully labeled in 5 rats under these conditions was found to be MCH+. Given the same profile of discharge of this MCH+ cell as that under the first condition and the lack of discharge during waking of the 2 cells under the different conditions, MCH+ cells were subsequently sought according to their special sleep–wake discharge profile in rats under normal feeding conditions (n = 27 cells successfully labeled in 17 rats).

Data Analysis. For analysis, units were selected that had been recorded for more than 5 min and during at least one episode of aW, SWS, and PS. Together with the synchronized video images of behavior, records of EEG and EMG were scored by 10-s epochs for sleep-waking state as described in refs. 1 and 2. Wake, SWS, and PS states were scored when characteristic EEG/EMG activity occupied >75% of the epoch; transitional stages into SWS and PS were scored when characteristic transitional activity or mixed activity occurred during the epoch. Active wake was scored when movement occurred during the wake epoch, as evident by phasic EMG activity along with video images, and theta EEG activity. The unit activity was subsequently analyzed per 10-s epoch in each sleep-waking state for average discharge rate (spikes per second) and instantaneous firing frequency by using the first modal peak of the interspike interval histogram (ISIH). Gamma (30–58 Hz) and delta (1–4.5 Hz) amplitude were measured per epoch along with EMG amplitude (30–100 Hz) for correlation with unit spike rate. Classification of units according to the state in which their maximal discharge rate occurred was performed by ANOVA followed by post hoc paired comparisons (1). All spikes were averaged across the recording for measurement of the spike duration (from first zero crossing on upward deflection to second zero crossing on second upward deflection on return to baseline, set at 10% of peak amplitude from zero). A total of 117 cells in 75 rats were recorded during one sleep–wake cycle and successfully labeled with Nb. From these, data of 12 cells had to be excluded because of an inadequate number of epochs in certain states for adequate spike sampling. Electrophysiological properties of cells were compared across groups using Student's *t* test and in relation to EEG and EMG using Pearson's correlation (Systat, v11).

Immunohistochemistry. After the recording and labeling of units, the rat was anesthetized with an overdose of sodium pentobarbital (Euthanyl, ≈100 mg/kg, i.p.) and perfused with a 4% paraformaldehyde solution. After immersion in 30% sucrose for 2–3 days, brains were frozen for storage and subsequent cutting into 25-μm-thick sections. For revelation of Neurobiotin, sections were incubated for 2.5 h in Cy2-conjugated streptavidin (1:1,000, Jackson ImmunoResearch). After location of an Nb-labeled cell, the relevant section was incubated overnight at room temperature in both rabbit anti-MCH antiserum (1:2,500, Phoenix Pharmaceuticals) and goat anti-Orx A antiserum (1:500, Santa Cruz Biotechnology) and subsequently for 2 h in Cy3-conjugated donkey anti-rabbit antiserum (1:1,000, Jackson) and Cy5-conjugated donkey anti-goat antiserum (1:800, Jackson). Nb-labeled cells were located by epifluorescence by using a Leica DMLB microscope and photographed by using a Nikon Eclipse E800 (Nikon Instruments) equipped with a digital camera (Optronics, Microfire S99808). The labeled cells were mapped onto a computer-resident atlas with the aid of Neurolucida (v7, MicroBrightField). From the 105 labeled cells for which full

electrophysiological data were available (above), data from 9 cells was excluded because the immunostaining was not considered definitively immunopositive or immunonegative for MCH, yielding data reported from a total of 96 Nb-labeled cells.

1. Lee MG, Manns ID, Alonso A, Jones BE (2004) Sleep-wake related discharge properties of basal forebrain neurons recorded with micropipettes in head-fixed rats. *J Neurophysiol* 92:1182–1198.
2. Lee MG, Hassani OK, Jones BE (2005) Discharge of identified orexin/hypocretin neurons across the sleep-waking cycle. *J Neurosci* 25:6716–6720.
3. Lee MG, Hassani OK, Alonso A, Jones BE (2005) Cholinergic basal forebrain neurons burst with theta during waking and paradoxical sleep. *J Neurosci* 25:4365–4369.
4. Georgescu D, *et al.* (2005) The hypothalamic neuropeptide melanin-concentrating hormone acts in the nucleus accumbens to modulate feeding behavior and forced-swim performance. *J Neurosci* 25:2933–2940.
5. Burdakov D, Gerasimenko O, Verkhratsky A (2005) Physiological changes in glucose differentially modulate the excitability of hypothalamic melanin-concentrating hormone and orexin neurons in situ. *J Neurosci* 25:2429–2433.
6. Silver IA, Erecinska M (1994) Extracellular glucose concentration in mammalian brain: continuous monitoring of changes during increased neuronal activity and upon limitation in oxygen supply in normo-, hypo-, and hyperglycemic animals. *J Neurosci* 14:5068–5076.
7. Bjursell M, *et al.* (2006) Melanin-concentrating hormone receptor 1 deficiency increases insulin sensitivity in obese leptin-deficient mice without affecting body weight. *Diabetes* 55:725–733.

A Firing during PS

PF

RS

EMG

Unit

(Average spike rate = 2 Hz)

EEG and EMG: 1mV
Unit: 2 mV

1 sec

B Instantaneous firing frequency during PS

17 ms (58.8 Hz)

Events

Interspike interval (msec)

C Spike duration

2.44 ms

Amplitude (mV)

msec

Fig. S1. Electrophysiological features used to characterize Nb+/MCH +, P-max neurons. (*A*) Polygraphic record of a typical MCH+ unit (c134u01) together with EEG (from PF and RS cortices) and EMG signals showing firing during one 10-s epoch of PS. Note that the unit fires in an irregular, phasic manner, often in double or triple spikes, although also single spikes sometimes separated by long intervals and yielding a low average spike rate of 2 Hz for this epoch (and 1.1 Hz across all epochs of PS for this cell). PF, prefrontal cortex; RS, retrosplenial cortex. (*B*) The instantaneous firing frequency of the same MCH+ unit (c134u01) during PS, as calculated from the first mode of the interspike interval histogram. Note that the modal interval is 17 ms which corresponds to an instantaneous firing frequency of 58.8 Hz that is much higher than the average discharge rate (of 1.1 Hz) and reflects the phasic discharge in spike doublets or triplets by the unit during PS. (*C*) Average spike duration of the same MCH+ unit (c134u01). Note the relatively broad action potential, which was measured as 2.44 ms (from the initial positive deflection to the return toward baseline after the negative deflection, setting the baseline around zero according to 10% of the positive peak amplitude).
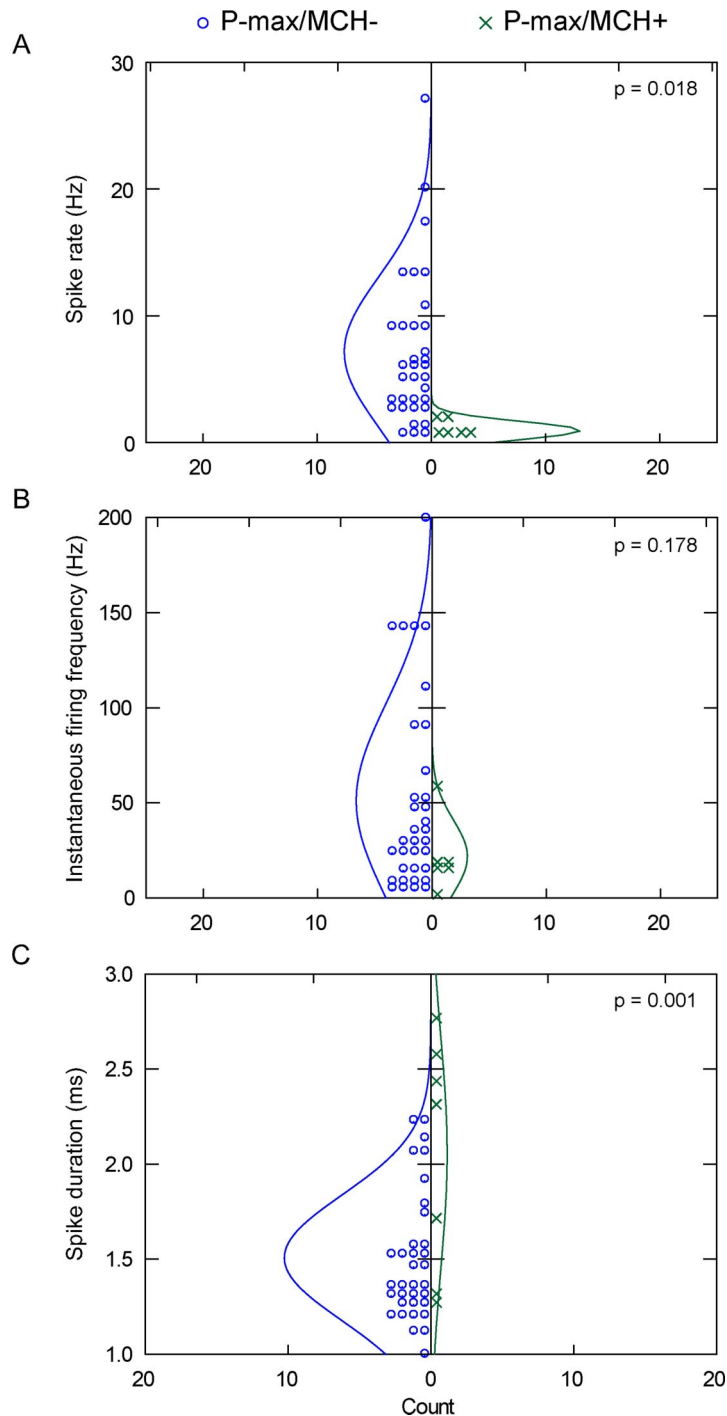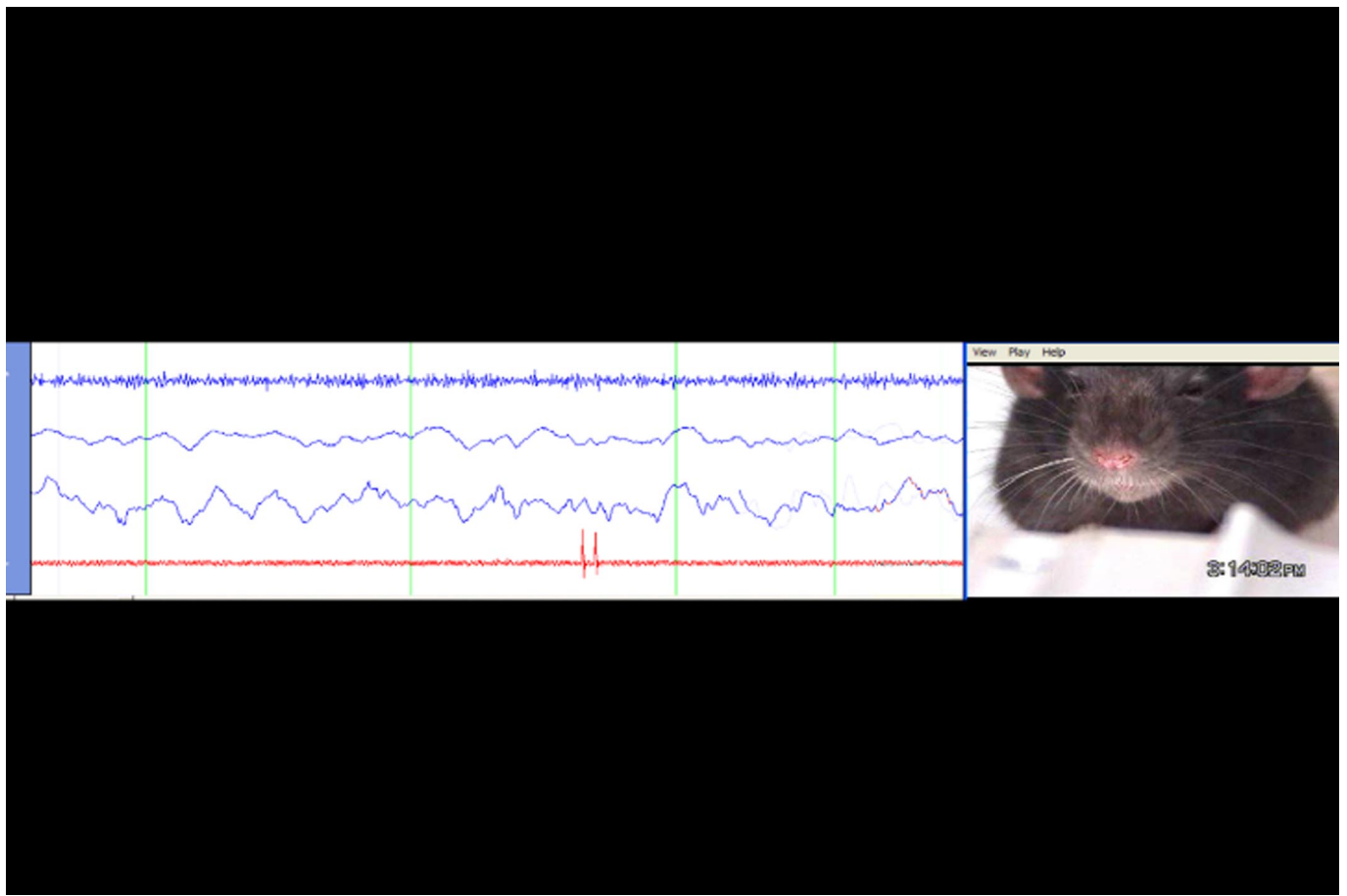
Fig. S2. Comparison of electrophysiological variables between Nb+/MCH+ and Nb+/MCH−, P-max neurons. (*A*) Average spike rate (Hz) during PS for MCH+ (1.1 ± 0.26 Hz, mean ± SEM, *n* = 6) vs. MCH− (7.14 ± 1.02 Hz, *n* = 34) P-max units. Note that although the mean spike rate is significantly lower for the MCH+ units (according to 2-sample *t* test, *P* = 0.018, df = 38), but that the values for MCH+ neurons overlap with a proportion of those for the MCH− cells. (*B*) Average instantaneous firing frequency for MCH+ (21.73 ± 7.86 Hz, *n* = 6) vs. MCH− (50.88 ± 8.79 Hz, *n* = 34) P-max units. Note that the mean frequency is insignificantly lower for the MCH+ cells (*P* = 0.178, df = 38), and the values for the MCH+ units overlap with a major proportion of those for MCH− cells. (*C*) Average spike duration for MCH+ (2.06 ± 0.23 ms, *n* = 7) vs. MCH− (1.51 ± 0.06 ms, *n* = 34) P-max cells. Note that the mean spike duration was significantly larger for the MCH+ than the MCH− cells (*P* ≤ 0.001, df = 39), but that the values for the MCH+ cells are highly variable and overlap with the major proportion of those for MCH− cells. Only for a subset of MCH+ cells with broad spike widths (>2.23 ms) is there no overlap with MCH− cells. Although selection of units according to the range of values for MCH+ cells by using any one variable would not allow their distinction from MCH− cells, selection using all 3 variables (spike rate, <1.95 Hz; instantaneous firing frequency, <58.83 Hz; spike duration, >1.27 ms), would provide a much greater probability of doing so (6 MCH+ and 1 MCH− or 6/7 = 86%) within our sample of P-max cells (*n* = 40). Nevertheless, only by juxtacellular labeling with immunohistochemical identification can the MCH+ cells be unequivocally identified.

Fig. S3. Comparison of electrophysiological variables among Nb+/Orx+, Nb+/MCH+, and Nb+/Orx−/MCH− neurons. (*A*) Average spike rate (Hz) for different cell groups during their respective maximal discharge states: Orx+ W-max cells (3.17 ± 0.79 Hz; mean ± SEM, *n* = 6), MCH+ P-max cells (1.1 ± 0.26 Hz, *n* = 6) and Orx−/MCH− cells (6.55 ± 0.8 Hz, *n* = 83). Note that the mean spike rate is similar for Orx+ and MCH+ neurons and that for neither is it significantly different (*P* > 0.05, df = 87) from the Orx−/MCH− cells due to the extensive overlap of the values. (*B*) Average instantaneous firing frequency of different cell groups during their respective maximal discharge states: Orx+ W-max cells (12.19 ± 2.9 Hz, *n* = 6), MCH+ P-max cells (21.73 ± 7.86 Hz, *n* = 6), and Orx−/MCH− cells (53.63 ± 5.89 Hz, *n* = 83) cells. Note that the mean frequency is similar for the Orx+ and MCH+ units and that for neither is it significantly different from Orx−/MCH− cells (*P* > 0.05, df = 87) because of the extensive overlap. (*C*) Average spike duration of different cell groups during their respective maximal discharge states: Orx+ W-max cells (2.02 ± 0.07 ms, *n* = 6), MCH+ P-max cells (2.06 ± 0.23 ms, *n* = 7), and Orx−/MCH− cells (1.49 ± 0.04 ms, *n* = 83). Note that the mean spike duration is similar for the Orx+ and MCH+ units and that for both, it is significantly larger than the Orx−/MCH− cells (*P* ≤ 0.001, df = 87). Neither Orx+ nor MCH+ cells could be distinguished from each other or from all Orx− or MCH− cells according to any one variable. Even by using all 3 variables, neither Orx+ nor MCH+ cells could be distinguished from all Orx− or MCH− cells with >60% probability. Only by respectively differentiating them as W-max and P-max could they be distinguished with a high probability (≥75%) from other W-max and P-max cells by using appropriate ranges for all 3 variables. Yet, really only by juxtacellular labeling with immunohistochemical identification can either cell group be unequivocally identified.

Movie S1. Simultaneous EEG/EMG/Unit along with behavioral video recording (of 30-s segment) showing discharge of MCH+ neuron (shown in Fig. 2) during slow wave sleep (SWS). Note that the cell discharged only occasionally with a few spikes during SWS marked by EEG high-voltage slow waves (1–4 Hz). The upper blue trace corresponds to EMG; the two middle blue traces correspond to EEG from prefrontal (PF) cortex and retrosplenial (RS) cortex; and the lower red trace corresponds to the unit discharge (Unit). Green vertical lines mark 1-s divisions.

Movie S1 (WMV)
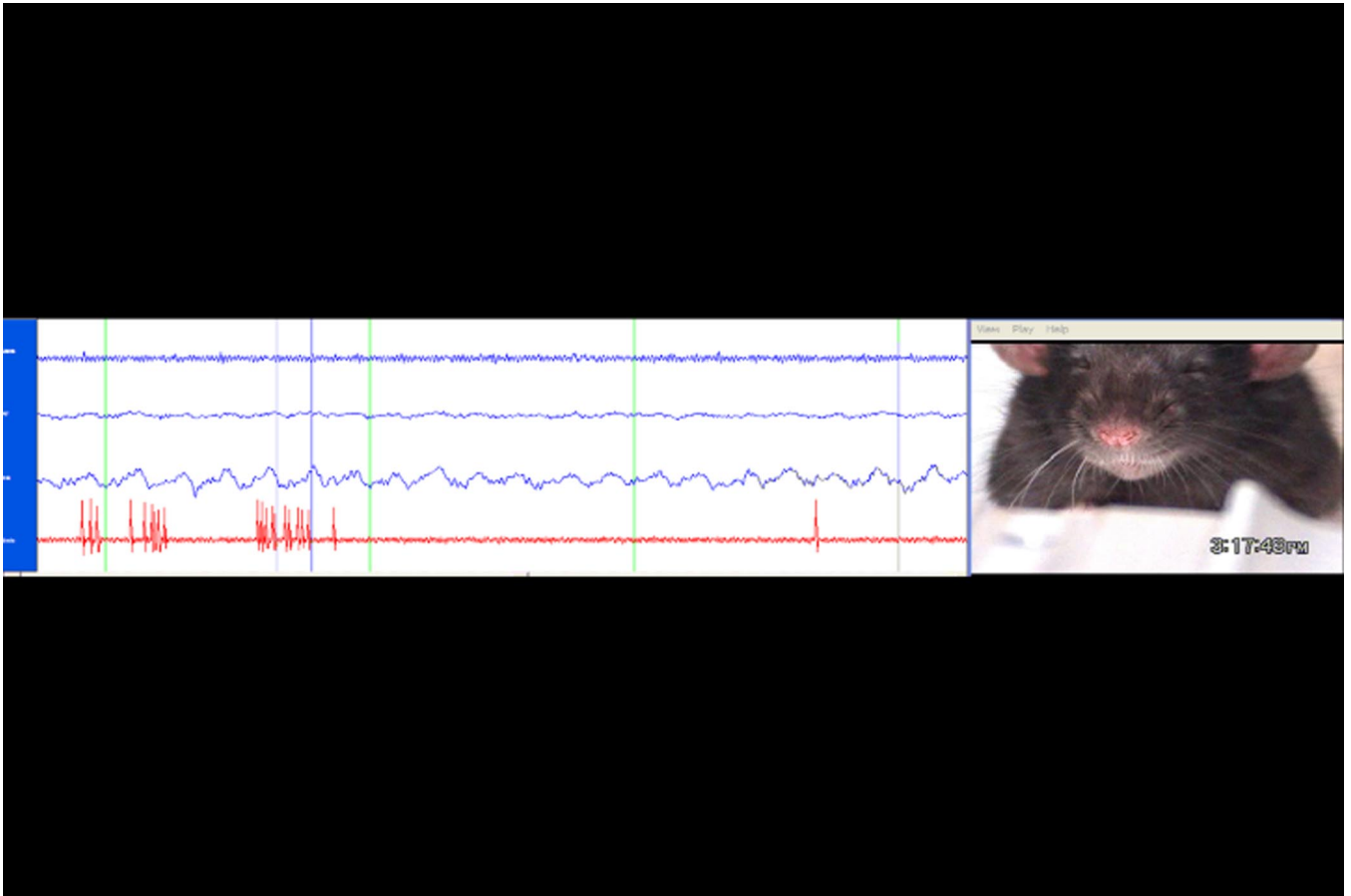
Movie S2. Simultaneous EEG/EMG/Unit along with behavioral video recording (of 30-s segment) showing discharge of MCH+ neuron (shown in Fig. 2) during paradoxical sleep (PS). Note that the cell discharged maximally but not continuously with doublets or groups of spikes during PS, which is marked by muscle atonia on the EMG and theta rhythm (4–9 Hz) on the EEG and is accompanied behaviorally by twitching of muzzle and whiskers.

[Movie S2 (WMV)](#)
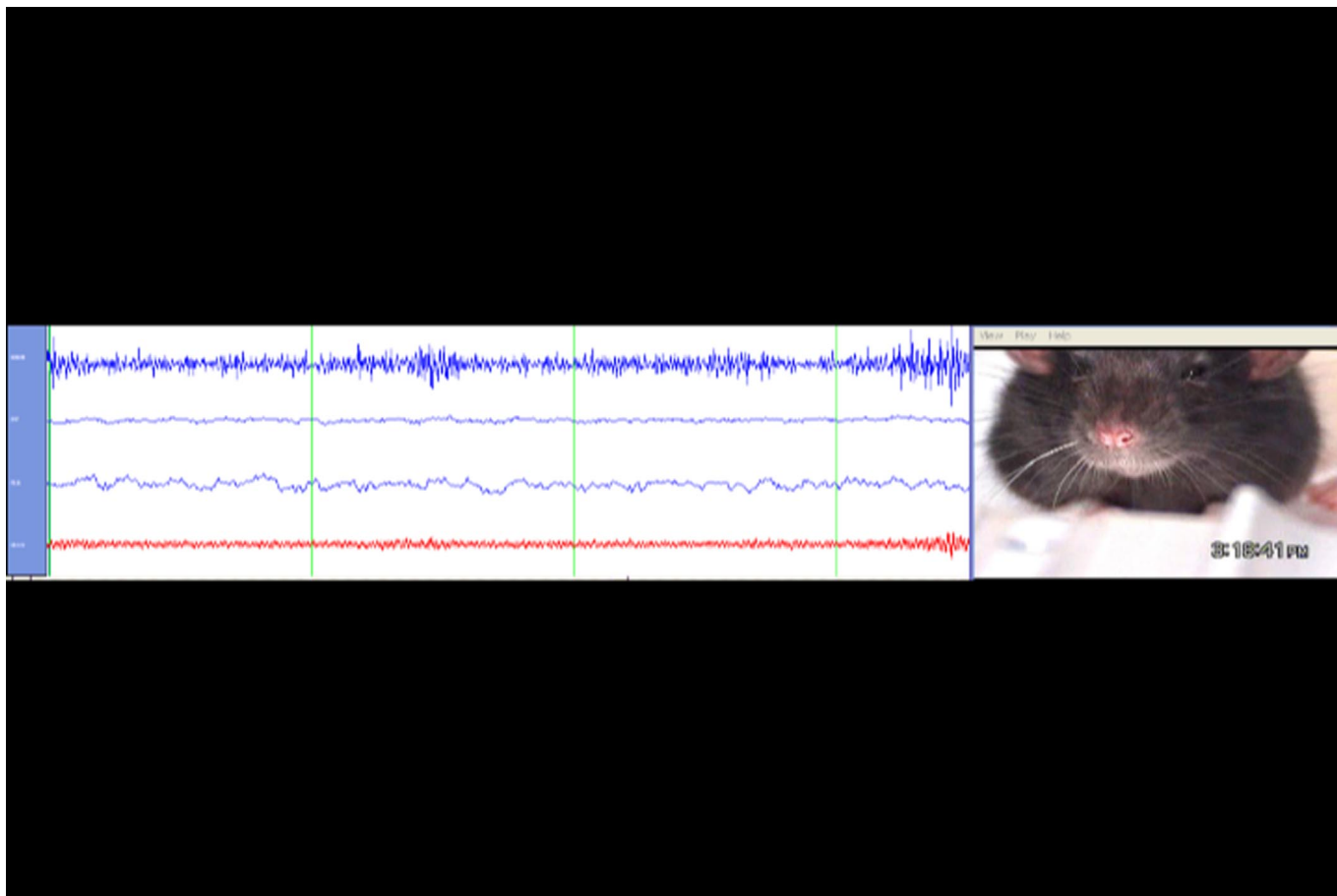
Movie S3. Simultaneous EEG/EMG/Unit along with behavioral video recording (of 30-s segment) of MCH+ neuron (shown in Fig. 2) during active wake (aW). Note that the cell remained silent during the entire period of aW marked by the presence of tonic and phasic muscle tone on the EMG along with occasional theta activity on the EEG during movements.

Movie S3 (WMV)